Semi-discrete Dynamics and Simulation of Peirce-Smith Converting

A. Navarra, G. Lemoine, N. Zaroubi and T. Marin

Abstract Peirce-Smith converting (PSC) is applied for roughly 50% of primary nickel and 70% of primary copper production. PSC cycles produce batches of iron-free sulfide matte (or blister copper, in the case of copper smelters), that are subject to further processing. However, the number of cycles that can be performed simultaneously is limited by the offgas handling system. Moreover, PSC suffers from variation in the yield and duration of the cycles. This variation is managed by conventional smelter designs, in which the upstream smelting capacity exceeds the nominal converting capacity; PSC is thus a major bottleneck in conventional nickel and copper smelters. Stabilization and standardization of PSC operations can therefore increase smelter throughput. The current paper presents a discrete event simulation (DES) framework to assist in smelter debottlenecking. It features random number generation to represent cycle variability, and time-adaptive finite differences to represent thermochemical complexity. Preliminary computations are presented.

Keywords Peirce-Smith converting · Discrete event simulation
Mass balance · Heat balance · Gibbs free energy balance

Introduction

Peirce-Smith converting (PSC) is applied for roughly 50% of primary nickel and 70% of primary copper production, which corresponds to 23 and 1270 kt, priced at 9200 USD/t and 5600 USD/t, respectively [1–3]. Moreover, PSC is often the main

A. Navarra (✉)
Universidad Católica del Norte, 0610 Angamos, Antofagasta, Chile
e-mail: anavarra@ucn.cl

G. Lemoine · N. Zaroubi
McGill University, 3610 University Street, Montreal, QC H3A 0C5, Canada

T. Marin
M4 Dynamics, 1 Younge Street, Suite 1801, Toronto, ON M5E 1W7, Canada

© The Minerals, Metals & Materials Society 2018

B. Davis et al. (eds.), *Extraction 2018*, The Minerals, Metals & Materials Series,
https://doi.org/10.1007/978-3-319-95022-8_22

bottleneck in conventional copper and nickel-copper smelters, as it sets the tempo for all subsequent operations. Thus improvements in PSC impact the overall productivity and sustainability of smelters. The potential for high impact developments is especially notable, considering the world-wide similarity of conventional smelters; improvements implemented in a specific smelter have been generalized and adapted to numerous other smelters. Such improvements have included the incorporation of tonnage oxygen for blast enrichment, and Gaspé punchers to periodically clear the tuyères [1]. Nonetheless, other potential improvements have merit, such as shrouded oxygen injection and waterless matte granulation [4–6], and have not been widely employed in conventional smelters, perhaps due to the lack of adequate quantitative tools to assess their system-wide benefits.

A PSC converting aisle consists of a parallel arrangement of converters, which functions together with the preceding smelting furnace (Fig. 1) to eliminate iron and sulfur from the iron-nickel-cobalt-copper sulfide feed. For nickel-copper smelters, the converted output is iron-free matte that is also known as Bessemer matte [7], and for copper smelters its so-called blister copper [8]; in both cases, the output requires further processing to eliminate deleterious minor elements, to retrieve valuable minor elements, and to cast nickel, cobalt and/or copper products. The oxidized sulfur leaves the bath in the form of SO_2, as part of the offgas. This offgas is essentially a mixture of N_2 and SO_2, but it typically carries some unreacted O_2 and considerable quantities of flue dust; for typical studies, it is usually a reasonable approximation to assume a single stable oxidized form of sulfur, namely SO_2. In contrast, there are two stable iron oxides, FeO and Fe_3O_4, which coexist within a fayalite or olivine slag [9]. The balance of FeO and Fe_3O_4 is quantified by the degree of iron oxidation $\alpha = Fe^{3+}/Fe^{2+}$ in the slag [10], which is computed through a Gibbs Free Energy balance, as discussed in the following section. Most importantly, α determines how much oxygen is required for each ton of feed, having a given composition; this ultimately determines the production rate of the entire smelter.

The current paper focuses on the development of a unified computational framework for nickel-copper and copper smelter analysis, and is part of a third installment (Fig. 2). The first installment was described in the first symposium on the Pyrometallurgy of Nickel and Cobalt in 2009 [5]. This work extended an operational cost model that had originally been developed for copper smelters [11];

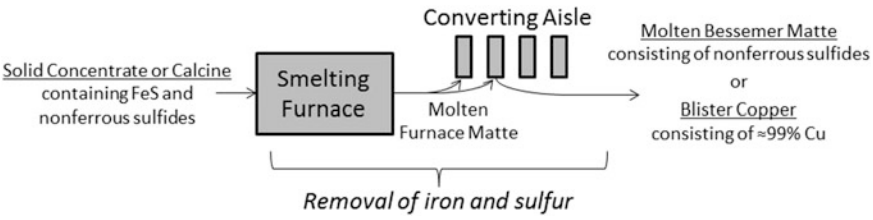

Fig. 1 Smelting furnace and converting aisle eliminate iron and sulfur, producing Bessemer matte in the case of nickel-copper smelters, and blister copper in the case of copper smelters

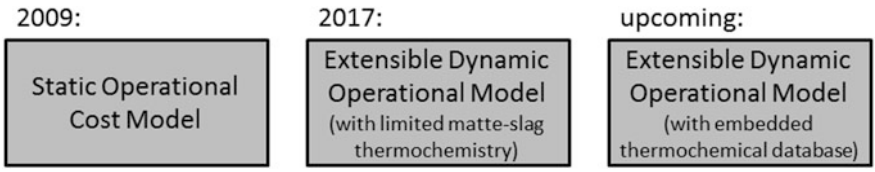

Fig. 2 Preparation of third installment of unified computational framework for analysis of nickel-copper and copper smelters

it included basic mass and heat balances that were static and deterministic, and thus did not adequately incorporate concepts of bottleneck management. (As described by the Theory of Constraints [12], temporary variations surrounding a bottleneck, can effectively diminish the overall throughput of the entire system). Additionally, α was artificially fixed, hence a lack of thermochemical realism. The second instalment was presented at the second symposium on Pyrometallurgy of Nickel and Cobalt in 2017, and later published in Canadian Metallurgical Quarterly [10]. Much of the underlying concepts of the 2009 model were transferred into a discrete event simulation (DES) framework, which now supports extensible dynamics modeling, and random number generation. However, the DES framework of 2017 only applied a Gibbs Free Energy balance for the degree of oxidation α of the smelting furnace, and not for the converting aisle.

The current paper is therefore to extend the DES framework, to adapt the approach of [10] which itself integrated earlier approaches of Goto [13], Kemori et al. [14], and Kyllo and Richards [15], and thus to incorporate dynamic α computations for each individual converter. Moreover, these developments involve dynamic temperature computations, which are related to the converter heat balance. This aspect is most notable to analyze the instalment of shrouded injectors and waterless matte granulation, thus to imbue PSC aisles with the advantages of SKS converters and Outotec-Kennecott flash converters, respectively. The shrouded injectors permit higher O_2 enrichment in the converters, such that less N_2 passes through the bath and into the offgas handling; the resulting offgas is thus richer in SO_2, which is favorable for acid production. However, increased enrichment tends to overheat the converters, unless the blastrate is diminished (which actually *decreases* the overall throughput, ironically), or unless sufficient solid feeds are available to replace the cooling effect of N_2. Indeed, the waterless matte granulation can be used to generate a stable supply of solid matte feed, and there is thus a synergistic benefit in simultaneously installing shrouded injection and waterless matter granulation. This approach for debottlenecking conventional smelters can allow conventional smelter designs to compete with both the SKS and Outotec-Kennecott designs. Nonetheless, smelters have been reluctant to experiment with this combination, perhaps because of a lack of computational tools to analyze the system-wide benefits.

Both the 2009 cost model and the 2017 DES framework presented a system-wide perspective. However, the DES framework is extensible, meaning that it can be developed in phases, throughout an engineering project. Even in the early phases of the project, the framework presents a holistic representation of the smelter, with interconnected components that represents the main aspects of smelter dynamics. However, as the project progresses, the framework accommodates increasing levels of detail for each of the most critical aspects for a given project. Beyond the incorporation of dynamic mass and heat balances, the framework has already been used in the scope of complex industrial problems, e.g. to optimize production scheduling [16], and to manage environmental risk due to meteorological uncertainty [17]. Indeed, to execute smelter improvement projects, the DES framework provides a starting point to build a virtual smelter, and then to incorporate sufficient detail to quantify the hypothetical benefits and risks of proposed operational and technological changes.

In summary, there are two avenues to extend the DES framework:

(1) Incorporate features that are universally relevant to all nickel-copper and copper smelters
(2) Customize the framework to address smelter-specific problems

The current paper works toward the former, as the issue of dynamic thermochemical fluctuations within converter cycles is common to all conventional nickel-copper and copper smelters. Beyond the scope of the current paper, there is an interest to develop a computer library that will connect the framework to state-of-the-art thermochemical databases, thus to address deeper problems involving slag chemistry, including minor element transport. The third installment of the framework will therefore provide an invaluable connection between the system-wide smelter metrics, and the inner functioning of individual furnaces.

Dynamic Themochemical Modeling of Converter Cycles

Peirce-Smith converters are operated in cycles, to produce batches of converted product [7, 8]. A cycle begins when an initially empty converter is filled to roughly half of its volume with matte, which is often combined with a quantity of silica flux as well as reverts, scrap and other cold charge. Oxygen-enriched air is then blown into the matte, as the iron combines with the incoming flux to form slag, and the corresponding sulfur is expelled as offgas; this process is known as the slag-blow, and it is halted intermittently, to skim away the accumulated slag, and possibly to introduce additional fresh ladles of matte and/or cold charges. Approximately all of the iron is eventually oxidized and skimmed away, thus signaling the end of the slag-blow. In the case of copper smelters, the blowing is continued, as the Cu_2S (a.k.a. white metal, [8]) is converted into blister copper; this is known as the copper-blow. Finally, the cycle is completed when the converter is emptied of its converted

product, be it iron-free matte in the context of nickel-copper smelting, or blister copper in the context of copper smelting.

Previously, the DES framework had considered only the discrete operational dynamics of converter cycles, including the initial charging and recharging events, as well as the skimming and emptying events. Indeed the durations of the blowing actions, as well as the quantities of incoming and outgoing material had all been treated as user parameters. The current developments are to explicitly represent thermochemical state variables PSC, to thus represent the evolving mass and heat content within each converter. This additional level of detail can allow the framework to evaluate (and eventually optimize) operating practices in response to short-term thermochemical variation. For example, if the temperature is rising slower than expected during a blowing action, then perhaps the skimming and recharging actions could be postposed, or perhaps certain types of cold charges could be conserved until a later charging event. Through simulation-based stochastic optimization [18], the framework can determine what operational triggers would favor one mitigating action over another.

For each converter, the framework now considers the variables listed in Table 1, in which

- n_{ij} is the number of moles of species or element i in phase j
- q_{Bath} is the heat content of the bath
- T_{Bath} is the common temperature of the slag and matte (i.e. $T_{\text{Bath}} = T_{\text{Matte}} = T_{\text{Slag}}$)
- α is the Fe^{3+}/Fe^{2+} ratio in the slag, a.k.a. the degree of oxidation

The internally computed variables T_{Bath} and α, are not explicitly represented as state variables, but are part of intermediate computations to compute rate-changes, as described below. Additionally, the new formulation considers several operational parameters,

- ϕ is the oxygen enrichment of the blast, expressed as a volume fraction
- $\dot{n}_{\text{O2, Blast}}$ is the molar rate at which oxygen is blown into the bath
- r_{Target} is the target SiO_2/Fe mass ratio within the slag
- T_{Blast} is the temperature of the incoming blast

Table 1 Classification of converter thermochemical state variables

Type of blow	Discretely dynamic state variables	Continuously dynamic state variables	Internally computed variables
Slag-blow in nickel-copper smelter	$n_{\text{NiS, Matte}}$, $n_{\text{CoS, Matte}}$ and $n_{\text{Cu2S, Matte}}$	$n_{\text{FeS, Matte}}$, $n_{\text{Fe,Slag}}$, $n_{\text{SiO2,Slag}}$ and q_{Bath}	T_{Bath} and α
Slag-blow in copper smelter	$n_{\text{Cu2S, Matte}}$	$n_{\text{FeS, Matte}}$, $n_{\text{Fe,Slag}}$, $n_{\text{SiO2,Slag}}$ and q_{Bath}	T_{Bath} and α
Copper-blow	none	$n_{\text{Cu2S, Matte}}$, $n_{\text{Cu, Blister}}$ and q_{Bath}	T_{Bath}

- T_{Flux} is the temperature of the incoming flux
- ϵ is the portion of incoming oxygen that reacts with the iron and sulfur rather, a. k.a. the oxygen efficiency
- $\dot{q}_{\text{Env}}$ is the rate of heat loss to the environment

some of which can be altered by a simulated operational policy, depending on the nature of the simulation. Indeed, $\dot{n}_{\text{O2, Blast}}$ can be computed from the blastrate and the oxygen enrichment ϕ. Within the scope of a simulation, these operational parameters are regarded as piecewise constant. In reality, certain of these quantities should actually be treated similarly to α and T_{Bath}, as internally computed state variables rather than operational parameters. In particular, ϵ and $\dot{q}_{\text{Env}}$ should depend on the thermochemical and fluid mechanical conditions within the bath; in the context of a smelter-specific study that emphasizes oxygen utilization or heat transfer, the DES can indeed be extended to incorporate submodels that describe the dynamic behavior of ϵ and/or $\dot{q}_{\text{Env}}$. Otherwise, ϵ can be set to between 85% and 100%, and $\dot{q}_{\text{Env}}$ can be set to between 2 and 4 MW, depending roughly on the configuration and size of the converter.

Historically, discrete event simulation only considered state variables that are updated at discrete points in time, i.e. at discrete events. As a first approximation for nickel-copper PSC, $n_{\text{NiS, Matte}}$, $n_{\text{CoS, Matte}}$ and $n_{\text{NiS, Matte}}$ are incremented only at charging events, and are decreased (to zero) only at the ends the cycles. More advanced implementations of DES allow the incorporation of state variables that have continuous dynamics, through the use of time-adaptive finite difference techniques, most notably the Runge-Kutta-Fehlberg method [19]; the incorporation of continuously changing variables into DES has been described the context of smelter dynamics by Navarra et al. [10]. The variables that are implemented with continuous dynamics (in addition to discrete dynamics) are more computationally demanding than those that only feature discrete dynamics. From the modeling perspective, however, the main difference is that the continuously changing variables require expressions for the rate of change.

The following formulas focus on the slag-blow, assuming a fayalite slag, considering that a similar approach can also be applied for olivine slag. (The copper-blow is far simpler than the slag-blow, because it is determined entirely from elemental mass balances that are algebraically decoupled from the heat balances). The rates of change of $n_{\text{Fe,Slag}}$, $n_{\text{FeS, Matte}}$ and $n_{\text{SiO2,Slag}}$ are determined through elemental mass balances that depend on α,

$$\dot{n}_{\text{Fe, Slag}} = \left(\frac{4+4\alpha}{6+7\alpha}\right)\epsilon\dot{n}_{\text{O2, Blast}} \tag{1}$$

$$\dot{n}_{\text{FeS, Matte}} = -\dot{n}_{\text{Fe, Slag}} \tag{2}$$

$$\dot{n}_{\text{SiO2, C1}} = \begin{cases} \left(\frac{r_{\text{Target}} M_{\text{Fe}}}{M_{\text{SiO2}}}\right)\dot{n}_{\text{Fe, Slag}}, & r = r_{\text{Target}} \\ 0, & r > r_{\text{Target}} \end{cases} \tag{3}$$

in which M_i is the molar mass of i, and r is the mass ratio of SiO_2/Fe in the slag, as calculated from the aforementioned state variables $r = (M_{SiO2} n_{SiO2,Slag})/(M_{Fe} n_{Fe,Slag})$. In Eqs. 2 and 3, the dependency on α is made explicit by substituting for $\dot{n}_{Fe,\,Slag}$. Equation 3 considers that r may exceed the target value r_{Target} following the addition of a cold charge, so that the continual addition of silica flux is halted until either $r = r_{Target}$ is reestablished through continued slag-blowing, or until the next skimming operation, which ever comes first. The case where $r < r_{Target}$ is not considered in Eq. 3, since it is presumed that the missing flux can be "rapidly" added, so that $r = r_{Target}$ is instantaneously reestablished. However, in a real smelter, it may take some time before the operators realize that there is a shortage of flux. Therefore, in an engineering project in which the flux response is critical, a submodel can be developed that describes the operators' behavior, including a probabilistic response time, and the risk of over- or under- compensating; otherwise, Eq. 3 is sufficiently detailed.

The rate of change in q_{Bath} is dependent on both T_{Bath} and α. The heat-rate balance is described by $\dot{q}_{Bath} = \dot{q}_{Blast} + \dot{q}_{Flux} - \dot{q}_{Offgas} - \dot{q}_{Env}$; in terms of molar flow rates,

$$\dot{q}_{Bath} = \left(\dot{n}_{N2,\,Blast}\Delta H_{N2,\,Blast} + \dot{n}_{O2,\,Blast}\Delta H_{O2,\,Blast}\right) + \dot{n}_{SiO2}\Delta H_{SiO2,\,Flux} - \left(\dot{n}_{N2,\,Offgas}\Delta H_{N2,\,Offgas} + \dot{n}_{O2,\,Offgas}\Delta H_{O2,\,Offgas} + \dot{n}_{SO2,\,Offgas}\Delta H_{SO2,\,Offgas}\right) - \dot{q}_{Env} \tag{4}$$

in which the enthalpies of formation ΔH_{ij} of species i in stream j takes the general form,

$$\Delta H_{ij} = \Delta H_i^{o} + a_i\left(T_j - T^{o}\right) + \frac{b_i}{2}\left(T_j^2 - T^{o2}\right) - c_i\left(\frac{1}{T_j} - \frac{1}{T^{o}}\right) + \frac{d_i}{3}\left(T_j^3 - T^{o3}\right) \tag{5}$$

in which in $(\Delta H_j^{o},\ a_j,\ b_j,\ c_j,\ d_j)$ are thermochemical constants [20], and $T^{o} = 298.15$ K is the Standard Temperature. For simplicity, SiO_2 has been assumed to be the only species within the flux and, conversely, flux is assumed to be the only continual stream of incoming SiO_2, either through a chute or Garr Gun [7, 8]. Also, $\dot{n}_{N2,\,Blast} = \dot{n}_{N2,\,Offgas}$ and $\dot{n}_{O2,\,Offgas}$ can be computed from operational parameters ϕ, $\dot{n}_{O2,\,Blast}$ and ϵ. Additional considerations are that the outgoing offgas has the same temperature as the bath,

$$T_{Offgas} = T_{Bath} \tag{6}$$

and that the oxidation of FeS is such that

$$\dot{n}_{SO2,\,Offgas} = \dot{n}_{Fe,\,Slag} \tag{7}$$

Within Eq. 4, the dependency on T_{Bath} is made explicit by applying Eqs. 5 and 6 to substitute for the $\Delta H_{i,Offgas}$ factors. The dependence on α is made explicit by

applying Eq. 3 to substitute for $\dot{n}_{SiO2}$, Eq. 7 to substitute for $\dot{n}_{SO2,\,Offgas}$, and finally by applying Eq. 1 to substitute for $\dot{n}_{Fe,\,Slag}$.

Equations 1–7 give the rate-changes of continuous variables as a function of (T_{Bath},α). However, (T_{Bath},α) are themselves determined by a nonlinear system of two equations and two unknowns, as described in the Appendix. These values are solved by Newton Method [21], with the kth iteration given by

$$\begin{pmatrix} T_{\mathrm{Bath}k} \\ \alpha_k \end{pmatrix} = \begin{pmatrix} T_{\mathrm{Bath},\,k-1} \\ \alpha_{k-1} \end{pmatrix} - \frac{1}{\frac{\partial f_H}{\partial T_{\mathrm{Bath}}}\frac{\partial f_G}{\partial \alpha} - \frac{\partial f_H}{\partial \alpha}\frac{\partial f_G}{\partial T_{\mathrm{Bath}}}} \begin{bmatrix} \frac{\partial f_G}{\partial \alpha} & -\frac{\partial f_H}{\partial \alpha} \\ -\frac{\partial f_G}{\partial T_{\mathrm{Bath}}} & \frac{\partial f_H}{\partial T_{\mathrm{Bath}}} \end{bmatrix} \begin{pmatrix} f_H \\ f_G \end{pmatrix} \tag{8}$$

in which all instances of f_H and f_G, and their partial derivatives, are evaluated at ($T_{Bath,k\text{-}1}$,$\alpha_{k\text{-}1}$); typical values for ($T_{Bath0,}$ α_0) can be (1473 K, 0.15). As described in the Appendix, f_H is proxy function, such that $f_H = 0$ if and only if the heat balance is satisfied; likewise f_G is a proxy function, such that $f_G = 0$ if and only if the Gibbs Free Energy balance is satisfied. Equation 8 captures the coupled nature of T_{Bath} and α.

The Newton iterations converge to a sufficient level of precision in usually fewer than ten iterations, and often fewer than five, giving values for T_{Bath} and α. These values are then used to update the rate-changes of Eqs. 1–7, which fit into a time-adaptive finite difference scheme to update the continuously dynamic state variables (Table 1), hence a dynamic representation of blowing actions. Intermittently, there are discrete instances in which material is charged or discharged from the converter. For simplicity, the skimmed slag is assumed to carry away the heat that corresponds to the bath temperature T_{Bath}, so that the skimming action does not alter T_{Bath}; however, within a more detailed smelter-specific project, it may be worthwhile to deduct an additional amount of heat that corresponds to the added radiation losses for having the hood lifted [7, 8]. In general, the formulation described in this section, and in the Appendix, provides a first approximation of PSC dynamics. Additional levels of detail are developed in phases, depending on the specific requirements of a particular project; this may involve modifying the equations described in this section, as well as developing submodels and subsubmodels. Ultimately, it is this extensible characteristic of DES that gives the framework its wide-ranging application.

Preliminary Computations

Equations 1–8 have been implemented in Matlab® to provide preliminary results (Fig. 3), prior to implementation into the DES framework; the parameters are described in Table 2, in which $w_{i\mathrm{FMatte}}$ is the weight fraction of i within the furnace matte. A total of 80 t of furnace matte is charged entirely at the beginning of the

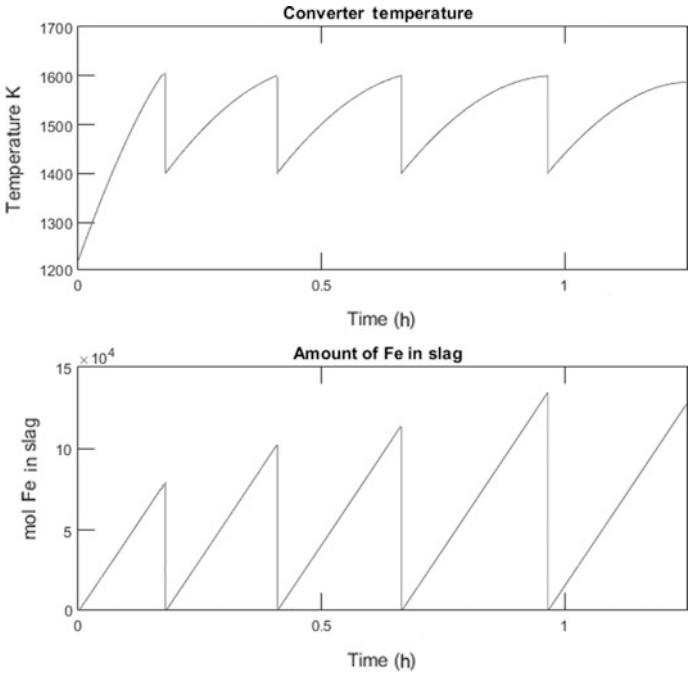

Fig. 3 Sample results displaying semi-discrete PSC dynamics

Table 2 Operational parameters

Parameter	Value		Parameter	Value	
ϕ	23		$\dot{q}_{\text{Env}}$	2	MW
$\dot{n}_{\text{O2, Blast}}$	360	vol.%O_2	T_{FMatte}	1225	K
r_{Target}	0.7	kmol/h	$w_{\text{FeS, FMatte}}$	39	%
T_{Blast}	298	K	$w_{\text{NiS, FMatte}}$	35	%
T_{Flux}	298	K	$w_{\text{CoS, FMatte}}$	4	%
ϵ	85	%	$w_{\text{Cu2S, FMatte}}$	22	%

cycle, at a temperature of 1225 K, and is subject to a simplified slag-blowing operation. The operation is decomposed into five blowing actions, which are punctuated by vertical decreases in temperature that are triggered when the temperature reaches 1600 K. These decreases consist of skimming actions, which are immediately followed by the loading of cold charges that consist entirely of granulated Bessemer matte; sufficient cold charge is added so that the temperature falls to 1400 K. The repeated addition of these cold charges causes the bath to gain

thermal inertia (heat capacity) as it accumulates nonferrous sulfides; this allows the blowing actions to become increasingly long, without overheating.

The sample computations in this section describe an unorthodox converter cycle that could not be applied without assuring a steady supply of granulated Bessemer matte. Such a supply of cold charges could be provided by waterless matte granulation [4], for example. A similar approach could be adapted for copper smelters if, prior to the beginning of certain copper-blows, a portion of the white metal is granulated to be used later as cold charge. Moreover, the system-wide effect of such a strategy cannot be quantified unless dynamic thermochemical PSC computations are integrated within a broader framework.

Future Work

Further development or extension of thermochemical capabilities of the DES framework can be achieved by using an add-in thermochemical library capable of carrying out complex multiphase Gibbs Energy Minimization for thermodynamic systems consisting of multiple components. This approach is particularly advantageous in the case of nonferrous pyrometallurgical processes, as these systems involve phases that are described by non-ideal solution models (see Appendix, or [10, 13–15]). More generally, a thermochemistry-based process simulation using Gibbs Energy Minimization reduces the number of assumptions, resulting in a very predictive and flexible tool. For example, the user does not need to explicitly specify the set of chemical reactions describing the process, nor the extent to which the reactions occur, nor the resulting phases.

A complete thermochemistry-based process simulator requires three main components, namely: (1) a robust Gibbs Energy Minimization algorithm for multiphase multi-component systems, (2) solution models that describe the various non-ideal mixtures in a wide range of temperature and compositions and (3) an extensive and critically assessed thermodynamic database defining the required parameters for the system of interest. Currently, M4D-DES™ is being developed by M4 Dynamics Inc. as an Add-in for a DES framework (Arena™). M4D-DES is based on ChemApp™, a robust and complete Gibbs Energy Minimizer library compatible with an extensive number of solution models and compatible with all the FactSage-Family of thermodynamic databases as well as with user-created databases. This will provide increased applicability and flexibility to the DES framework described here. For example the extended framework will be able to analyze transport of minor elements, extend the number of system components of the system, and provide possibilities to better analyze the impact of different feed sources on the smelter throughput, including economic and environmental impacts.

Appendix: Proxy Functions for Heat and Gibbs Free Energy Balances

Equation 8 describes the Newton iterations that are used to simultaneously solve for the temperature of the bath T_{Bath} and the degree of oxidation of the slag α. These iterations are configured so as to simultaneously balance the heat and Gibbs Free Energy, hence two equations and two unknowns.

Firstly, the heat balance is given by $q = \sum_{j \in \{\text{Matte, Slag}\}} \sum_{i \in \mathcal{S}_j} n_{ij} \Delta H_{ij}$ in which $\mathcal{S}_j$ is the set of species in bath stream j; equivalently the heat balance can be expressed in terms of a proxy function $f_{\text{H}} \equiv \sum_{j \in \{\text{Slag, Matte}\}} \sum_{i \in \mathcal{S}_j} n_{ij} \Delta H_{ij} - q$, such that the $f_{\text{H}} = 0$ if and only if the heat balance is satisfied. Following a sequence of substitutions using Eq. 5, and several additional algebraic manipulations, the proxy function can be expressed explicitly in terms of T_{Bath} and α, as required by Newton's method.

$$
\begin{aligned}
f_{\text{H}}(T_{\text{Bath}}, \alpha) = {} & \left(\Sigma n_{ij} \Delta H_i^{\text{o}}\right) + \left(\Sigma n_{ij} a_i\right)\left(T_{\text{Bath}} - T^{\text{o}}\right) + \frac{1}{2}\left(\Sigma n_{ij} b_i\right)\left(T_{\text{Bath}}^2 - T^{\text{o}2}\right) - \left(\Sigma n_{ij} c_i\right)\left(\frac{1}{T_{\text{Bath}}} - \frac{1}{T^{\text{o}}}\right) \\
& + \frac{1}{3}\left(\Sigma n_{ij} d_i\right)\left(T_{\text{Bath}}^3 - T^{\text{o}3}\right) \\
& + \left(\frac{n_{\text{Fe, Slag}}}{1+\alpha}\right)\left[\begin{array}{l} \Delta H_{\text{FeO}}^{\text{o}} + a_{\text{FeO}}\left(T_{\text{Bath}} - T^{\text{o}}\right) + \frac{b_{\text{FeO}}}{2}\left(T_{\text{Bath}}^2 - T^{\text{o}2}\right) \\ \quad - c_{\text{FeO}}\left(\frac{1}{T_{\text{Bath}}} - \frac{1}{T^{\text{o}}}\right) + \frac{d_{\text{FeO}}}{3}\left(T_{\text{Bath}}^3 - T^{\text{o}3}\right) \end{array}\right] \\
& + n_{\text{Fe, Slag}}\left(\frac{\alpha}{1+\alpha}\right)\left[\begin{array}{l} A + B\left(T_{\text{Bath}} - T^{\text{o}}\right) + C\left(T_{\text{Bath}}^2 - T^{\text{o}2}\right) \\ + D\left(\frac{1}{T_{\text{Bath}}} - \frac{1}{T^{\text{o}}}\right) + E\left(T_{\text{Bath}}^3 - T^{\text{o}3}\right) \end{array}\right] - q
\end{aligned}
\tag{9}
$$

in which the summations are taken over $(i, j) \in \{$(FeS, Matte), (NiS, Matte), (CoS, Matte), (Cu_2S, Matte), (SiO_2,Slag) $\}$, and the constant coefficients (A, B, C, D, E) are given in Table 3. Given Eq. 9, it is straightforward to obtain expressions for $\frac{\partial f_{\text{H}}}{\partial T_{\text{Melt}}}$ and $\frac{\partial f_{\text{H}}}{\partial \alpha}$, which are also present in Eq. 8.

Navarra et al. [10] relied on a proxy function f_{G} that was expressed explicitly as a function of α. The approach has now been slightly modified so that f_{G} can be expressed explicitly as a function of T_{Bath}, as well as α.

Table 3 Coefficients for Eq. 9

A	B	C	D	E
$\frac{1}{2}\left(\Delta H_{\text{Fe3O4}}^{\text{o}} - \Delta H_{\text{FeO}}^{\text{o}}\right)$	$\frac{1}{2}\left(a_{\text{Fe3O4}} - a_{\text{FeO}}\right)$	$\frac{1}{4}\left(b_{\text{Fe3O4}} - b_{\text{FeO}}\right)$	$-\frac{1}{2}\left(c_{\text{Fe3O4}} - c_{\text{FeO}}\right)$	$\frac{1}{6}\left(d_{\text{Fe3O4}} - d_{\text{FeO}}\right)$

$$f_G(T_{Bath}, \alpha) = \prod_{l=1}^{3} (A_l + B_l\alpha)^{C_l + D_l/T_{Bath}} - \prod_{l=4}^{9} (A_l + B_l\alpha)^{C_l + D_l/T_{Bath}} \quad (10)$$

in which the coefficients (A_l, B_l, C_l, D_l) are given in Table 4. Considering that D_l is zero for all but two factors, Eq. 10 can also be expressed as

$$f_G(T_{Bath}, \alpha) = \prod_{l=1}^{2} (A_l + B_l\alpha)^{C_l} (A_3 + B_3\alpha)^{15430/T_{Bath}} - \prod_{l=4}^{8} (A_l + B_l\alpha)^{C_l} (A_9 + B_9\alpha)^{15430/T_{Bath}}$$

which is helpful for finding an expression for $\frac{\partial f_H}{\partial T_{Melt}}$; to find an expression for $\frac{\partial f_G}{\partial \alpha}$ it is simpler to work directly with Eq. 10.

Within Table 4, R denotes the ideal gas constant, and $X_{FeS,\ Matte}$ is the molar fraction of FeS within the matte, given by $X_{FeS,\ Matte} = n_{FeS,Matte} / (n_{FeS,Matte} + n_{NiS,\ Matte} + n_{CoS,\ Matte} + n_{Cu2S,\ Matte})$. Additionally, Table 4 includes ΔH_0 and ΔS_0 which are the enthalpy and entropy of the following equilibrium,

$$FeS_{(Matte)} + 3Fe_3O_{4(Slag)} \leftrightarrow 10FeO_{(Slag)} + SO_{2(Offgas)}$$

Indeed, the approach of Navarra et al. [10], and hence Eq. 10, is based on this equilibrium, using the expressions of Goto [13] and Kemori et al. [14] for the activity coefficients of FeS, FeO and Fe_3O_4. These expressions had originally been developed for copper smelters, but were successfully adapted and tested for nickel-copper smelters [15].

Table 4 Coefficients for Eq. 10

l	A_l	B_l	C_l	D_l
1	1	1	1	0
2	2	-1	10	0
3	$\left(2.44 - 0.4\left(\frac{n_{SiO2,\ Slag}}{n_{Fe,\ Slag}}\right)\right)$	$-\left(1.42 + 0.4\left(\frac{n_{SiO2,\ Slag}}{n_{Fe,\ Slag}}\right)\right)$	0	15430
4	$X_{FeS,\ Matte} e^{\frac{\Delta S_0}{R}}$	0	1	0
5	0	1	3	0
6	$\left(\frac{3-\phi\epsilon}{2\phi\epsilon}\right)$	$\left(\frac{7-3\phi\epsilon}{4\phi\epsilon}\right)$	1	0
7	$\left(1.38 + 12.28\left(\frac{n_{SiO2,\ Slag}}{n_{Fe,\ Slag}}\right)\right)$	$\left(56.8 + 12.28\left(\frac{n_{SiO2,\ Slag}}{n_{Fe,\ Slag}}\right)\right)$	3	0
8	$2\left(1 + \left(\frac{n_{SiO2,\ Slag}}{n_{Fe,\ Slag}}\right)\right)$	$2\left(\frac{n_{SiO2,\ Matte}}{n_{Fe,\ Slag}}\right)$	4	0
[a]9	$2\left(1 + \left(\frac{n_{SiO2,\ Slag}}{n_{Fe,\ Slag}}\right)\right)K$	$2\left(\frac{n_{SiO2,\ Slag}}{n_{Fe,\ Slag}}\right)K$	0	15430

[a]in which $K = e^{-\Delta H_0/15430R}(0.54 + 0.52X_{FeS,\ Matte} + 1.4X_{FeS,\ Matte} \ln X_{FeS,\ Matte})^{1458/15430}$

References

1. Price T, Harris C, Hills S, Boyd W, Wraith A (2009) Peirce-smith converting: another 100 years? In: Paper presented at the 138th TMS annual meeting, San Francisco, California, 15–19 February 2009
2. McRae M (2018) Nickel. Minerals Commodity Summary. United States Geological Survey, Washington DC, pp 112–113
3. Flanagan D (2018) Copper. Minerals Commodity Summary. United States Geological Survey, Washington DC, pp 52–53
4. Mucciardi F, Palumbo E, Jin N (1999) A waterless caster for matte/slag granulation. In: Paper presented at the 4th international copper conference, Phoenix, Arizona 10–13 October 1999
5. Navarra A, Kapusta J (2009) Decision-making software development for incremental improvement of nickel matte conversion. In: Paper presented at the 48th annual conference of metallurgists of CIM, Sudbury, Ontario, 23–26 August 2009
6. Chibwe D, Akdogan G, Bezuidenhout G, Kapusta J, Bradshaw S, Eksteen J (2015) Sonic injection into a PGM Peirce-Smith converter: CFD modelling and industrial trials. J S Afr I Min Metall 115:115–349
7. Crundwell F, Moats M, Ramachandran V, Robinson T, Davenport W (2011) Converting—final oxidation of iron from molten matte. In: Chapter 19 in: Extractive metallurgy of nickel, cobalt and platinum group metals. Elsevier, Oxford, pp 233–246
8. Schlesinger M, King M, Sole K, Davenport W (2011) Converting of copper matte. In: Chapter 8 in: extractive metallurgy of copper. Elsevier, Oxford, p. 127–153
9. Ramirez C, Ruz P, Riveros G, Warczok A, Treimer R (2009) Chrome-magnesite refractory corrosion with olivine slag of high cuprous oxide content. In: Paper presented at the 138th TMS annual meeting, San Francisco, California, 15–19 February 2009
10. Navarra A, Valenzuela F, Cruz R, Arrancibia C, Yañez R, Acuña C (2018) Incorporation of matte-slag thermochemistry into sulphide smelter discrete event simulation. CMQ 57(1):70–79
11. Ng K, Kapusta J, Harris R, Wraith A, Parra R (2005) Modeling Peirce-Smith converter operating costs. JOM 57(7):52–57
12. Dettmer H (2007) Introduction to the theory of constraints. In: Chapter 1 in: the logical thinking process: a systems approach to complex problem solving. ASQ Quality Press, Milwaukee, p. 3–30
13. Goto S (1974) Equilibrium calculations between matte, slag and gaseous phases in copper smelting. In: Paper presented at the annual meeting of the institution of mining and metallurgy, Brussels, Belgium, 11–13 February 1974
14. Kemori N, Kimura T, Mori Y, Goto S (1987) An application of Goto's model to a copper flash smelting furnace. In: Presented at the annual meeting of the institution of mining and metallurgy, London, England, 21–23 September 1987
15. Kyllo A, Richards G (1991) A mathematical model of the nickel converter: part 1—model development and verification. Metall Trans B 22(2):153–161
16. Navarra A (2016) Automated scheduling and scientific management of copper smelters. T I Min Metall C 125(1):39–44
17. Navarra A, Marambio H, Oyarzún F, Parra R, Mucciardi R (2016) System dynamics and discrete event simulation of copper smelters. Miner Metall Process 34(2):96–106
18. Kleijnen J, Wan J (2007) Optimization of simulated systems: OptQuest and alternatives. Simul Model Pract Th 15(3):354–362
19. Kelton W, Sadowski R, Swets N (2010) Continuous and combined discrete/continuous models. In: Chapter 11 in: Modeling and simulation of discrete-event systems. Wiley, Hoboken, New Jersey, pp 473–512
20. Liley P, Thomson G, Daubert T, Buck E (1997) Physical and chemical data. Part 2 in: Perry's Chemical Engineers' Handbook. McGraw-Hill, New York, pp 1–204
21. Burden R, Faires J, Burden A (2016) Numerical solutions of nonlinear systems of equations. In: Chapter 10 in: numerical analysis. Cengage Learning, Boston, Massachusetts, pp 641–683